Journal of Ethnopharmacology 320 (2024) 117132

Contents lists available at ScienceDirect

Journal of Ethnopharmacology

journal homepage: www.elsevier.com/locate/jethpharm

Orthosiphon aristatus (Blume) Miq. Extracts attenuate Alzheimer-like pathology through anti-inflammatory, anti-oxidative, and β-amyloid inhibitory activities

Kuang-Hsing Chiang [a,b,c,d], Tain-Junn Cheng [e,f], Wei-Chih Kan [g,h], Hsien-Yi Wang [g,i], Jui-Chen Li [j], Yan-Ling Cai [k], Chia-Hui Cheng [k], Yi-Chien Liu [k], Chia-Yu Chang [e,l,*], Jiunn-Jye Chuu [j,k,**]

[a] Taipei Heart Institute, Taipei Medical University, Taipei 11031, Taiwan
[b] Division of Cardiology and Cardiovascular Research Center, Taipei Medical University Hospital, Taipei 11031, Taiwan
[c] Department of Internal Medicine, School of Medicine, College of Medicine, Taipei Medical University, Taipei 11031, Taiwan
[d] Graduate Institute of Biomedical Electronics and Bioinformatics, National Taiwan University, Taipei 10617, Taiwan
[e] Department of Neurology, Chi Mei Medical Center, Yong-Kang District, Tainan 71004, Taiwan
[f] Department of Occupational Medicine Chi Mei Medical Center, Yong-Kang District, Tainan 71004, Taiwan
[g] Division of Nephrology, Chi Mei Medical Center, Yong-Kang District, Tainan 71004, Taiwan
[h] Department of Medical Laboratory Science and Biotechnology, Chung Hwa University of Medical Technology, Tainan 71703, Taiwan
[i] Department of Sport Management, College of Leisure and Recreation Management, Chia Nan University of Pharmacy and Science, Tainan 71710, Taiwan
[j] Pharmacy Department, Wei-Gong Memorial Hospital, Miaoli 35159, Taiwan
[k] Department of Biotechnology and Food Technology, College of Engineering, Southern Taiwan University of Science and Technology, Tainan 71005, Taiwan
[l] Center for General Education, Southern Taiwan University of Science and Technology, Tainan 71005, Taiwan

ARTICLE INFO

Handling Editor: Dr. P. Fernandes

Keywords:
Orthosiphon aristatus (OA)
Alzheimer's disease (AD)
Beta-amyloid (Aβ)
Neurofibrillary tangles (NFT)

ABSTRACT

Ethnopharmacological relevance: *Orthosiphon aristatus* (Blume) Miq. (OA) is a traditional folk-herb, which is usually used to treat acute and chronic nephritis, epilepsy, cystitis, and other diseases. Phenols and flavonoids are the main active compound compounds of OA, with proven anti-inflammatory and antioxidant activities.

Aims of this study: Based on evidenced therapeutic activities, we aimed to investigate the impact of OA on Alzheimer's disease (AD) which is the most common age-related neurodegenerative disease, and the pathological features include accumulation of beta-amyloid (Aβ) and neurofibrillary tangles (NFT).

Materials and methods: OA was extracted with water, methanol, chloroform, and ethyl acetate, and determined its total flavonoid and phenolic contents. Initially, $A\beta_{1\text{-}42}$ based cytotoxicity was induced in BV2 cells and C6 cells to investigate the therapeutic impact of OA therapy by MTT, RT-PCR, Western blot, and ELISA. Further, $A\beta_{1-42}$ Oligomer (400 pmol)-induced AD mice model was established to evaluate the impact of OA extract on improving learning and memory impairment.

Results: The results showed that the extract of OA could increase cell survival, inhibit the expression of TNF-α, IL-6, IL-1β, COX-2, and iNOS, and increase BDNF levels. We infer that the OA extract may attenuate Aβ-induced cytotoxicity by retarding the production of inflammatory-related factors. In the animal behavior test, the number of mice entering darkroom and the time of arriving at the platform were significantly reduced, indicating the learning and memory-improving ability of OA extract.

Conclusions: These findings imply that the OA ethanolic extract demonstrated an improving effect on memory and hence could serve as a potential therapeutic target for the treatment of neurodegenerative diseases like AD.

* Corresponding author. Department of Neurology, Chi Mei Medical Center, Yong-Kang District, Tainan 71004, Taiwan.
** Corresponding author. Department of Biotechnology and Food Technology, College of Engineering, Southern Taiwan University of Science and Technology, Tainan 71005, Taiwan.
E-mail addresses: chiayu.chang7@msa.hinet.net (C.-Y. Chang), jjchuu@stust.edu.tw (J.-J. Chuu).

https://doi.org/10.1016/j.jep.2023.117132
Received 6 July 2023; Received in revised form 29 August 2023; Accepted 4 September 2023
Available online 11 September 2023
0378-8741/

1. Introduction

Alzheimer's disease (AD) is a prevalent neurodegenerative disorder among the aging population that triggers slow degeneration of brain cells, causing a decline in cognitive activity and dementia (Breijyeh and Karaman, 2020; Scheltens et al., 2021a,b). The increase in the aging population has escalated the number of Alzheimer's patients around the globe and unwarranted pressure on the economy and healthcare sector. As per recent reports, the number of Alzheimer's patients will reach up to 50 million by 2050 and 13.8 million by 2060 in the United States (US) alone (2021; Zhang et al., 2021). AD among the aging population severely impacts health, brain function specifically memory, and quality of life (QoL) (2021; Medeiros et al., 2011; Weidner and Barbarino, 2019). Moreover, dementia cases have considerably increased in Pacific countries such as China (5%), Japan (2%), and Taiwan (4%) (Khazaei et al., 2021). Notably, in Taiwan, a 6.7 times increase has been observed resulting in 300,000 dementia patients in the past three decades (Kao et al., 2022). Moreover, the cases of AD are more prevalent among Taiwanese women in comparison to males in the 75–84 years population and the prevalence rate increased from 5.63/1000 persons-year in 2005 to 8.17/1000 persons-year in 2010 (Hung et al., 2016). Along with cognitive impairment, other symptoms such as anxiety, interrupted sleep, impaired appetite, metabolic disorders, apathy, and depression appear as comorbid or isolated events in AD patients (Burke et al., 2018; Chatterjee et al., 2016; De Felice and Lourenco, 2015; Figueiro et al., 2014; Frozza et al., 2018; Ishii and Iadecola, 2015; Lanctôt et al., 2017). The presence of amyloid-β (Aβ) plaques, neurofibrillary tangles, and loss of neurons and synapses are characteristically associated with cognitive impairment and progression of AD (Kocahan and Doğan, 2017).

Further, at the initial stage, a reduction in cerebral blood flow (CBF) occurs due to oligomeric Aβ mediated constriction of capillaries (Korte et al., 2020). Augmentation of aggregated Aβ plaque due to improper processing of amyloid precursor proteins (APP) and neurofibrillary tangles (NFTs) of hyperphosphorylated tau protein are considered major pathological causes of AD and brain atrophy (Ashrafian et al., 2021; Korte et al., 2020; Medeiros et al., 2011; Sun et al., 2015). In addition, the presence of oxidative damage and active inflammatory cells is also associated with β plaque and NFTs (Sun et al., 2015). The proper APP cleavage generates C99 fragments which are further breakdown into $A\beta_{40}$ and $A\beta_{42}$, and the misfolding of $A\beta_{42}$ causes aggregation of β-plaque in the neocortex, hippocampus, and cerebrovasculature regions (Bloom, 2014; Chen et al., 2017; Viswanathan and Greenberg, 2011). The cumulative effect of reduction of $A\beta_{40}$ and elevation of $A\beta_{42}$ level in senile plaque results in neuroinflammation, insulin resistance, mitochondrial dysfunction, metabolic dysregulation, altered cholesterol homeostasis, and apoptosis of brain cells (Heneka et al., 2015; Jeremic et al., 2021; Neniskyte et al., 2011). The aggregated Aβ instigate the synthesis of reactive oxygen species (ROS) which causes oxidative damage not only to the amyloid peptide but also to other macromolecules such as protein, lipids, DNA, and functional enzymes like creatine kinase and glutamine synthetase resulting in loss of membrane integrity, cognitive and neuronal function (Castegna et al., 2002; Cheignon et al., 2018; Huang et al., 2004; Sun et al., 2015). Moreover, the oxidation of lipids by ROS results in the accumulation of peroxidized lipids in the white and grey matter of the brain resulting in neurotoxicity, brain lesions, loss of Ca^{2+} homeostasis, and inhibition of neuronal cell signaling (Benseny-Cases et al., 2014; Ezeani and Omabe, 2016; Mark et al., 1995; Peña-Bautista et al., 2019; Varadarajan et al., 2000; Zarrouk et al., 2015). Thus, to overcome the limitation of current therapy and to provide alternative therapy more therapeutic candidates are being explored.

Orthosiphon Aristatus (Blume) Miq. is a medicinal herb that is traditionally employed in the treatment of diabetes and kidney diseases in Southeast Asia (Chua et al., 2018). In Taiwan, the application of OA has been described as a food ingredient that could be used for the treatment of renal inflammation and dysuria (Chau and Wu, 2006). *Orthosiphon Aristatus* (OA) is also a widely recognized medicinal plant in Thai traditional medicine and holds significant popularity for its effectiveness in treating dysuria. In a seminal study, OA extract obtained using hexane revealed high potential in the treatment of dysuria (Ngamrojanavanich et al., 2006). Studies have also reported it as a traditional remedy for central nervous system disorders including epilepsy, a brain disorder characterized by seizures (Chung et al., 2020a,b; Hossain and Mizanur Rahman, 2015). AD exhibits heightened vulnerability to seizures and silent epileptiform activity, arising from an imbalance in excitatory and inhibitory neuronal signals, which can elevate cognitive decline (Kang, 2021; Vossel et al., 2017). This underscores the need for OA to mitigate the pathologic characteristics of AD. The reported phytochemical components of OA include polyphenols, phenolic acids, terpenes, and flavones such as rosmarinic, caffeic acid, eupatorine, sinensetin, salvigenin, and 3′-hydroxy-5,6,7,4′- tetramethoxyflavone, orthosiphols R-T, norstaminols B and C, secoorthosiphols A-C etc. These bioactive compounds have demonstrated with analgesic, antipyretic, antioxidant, antimicrobial, anti-inflammatory, antiproliferative, diuretic, anti-urolithic, norexic, diuretic, hypouriceamic, antiurolithic, hepatoprotective, antihypertensive, nephroprotective, gastroprotective, cardiovascular-protective, hypolipidaemic, anti-obesity, hypoglycaemic, anti-angiogenic and anti-sebum potential (Alshehade et al., 2022; Chung et al., 2020c; Lim and Chua, 2021; Mohd Bohari et al., 2021; Rocha et al., 2015; Son et al., 2011).

Thus, considering these above-mentioned therapeutic potential of OA including central nervous system, we aimed to offer a scientific perspective to traditional medicinal practices and designed this experimental study to investigate the possible beneficial effect of OA extracts on attenuating β-amyloid-induced cellular toxicity *in vitro* in glial cell lines and impaired learning and memory in mice.

2. Materials and methods

2.1. Plant materials

Orthosiphon Aristatus (Blume) Miq. was procured from Guohua Street-Shuixiangong Qingcao Store, Tainan City), which authenticated by Professor Jiunn-Jye Chuu (Department of Biotechnology and Food Technology, College of Engineering, Southern Taiwan University of Science and Technology, Taiwan). The plant name has been checked with http://www.theplantlist.org (accessed on 17 May 2023).

2.2. Chemicals and reagents

Ethyl acetate, Ethyl acetate, Methanol, and Chloroform are produced by GRAND Chemical Co., Ltd. (Miaoli, ZMI, Taiwan). Mouse BV2 microglial cells were purchased from American Type Culture Collection (Manassas, Va, USA). Rat C6 glioma cell was purchased from the Food Industry Research and Development Institute (Taiwan). Ham's F-10 medium was purchased from SIGMA (Saint Louis, MO, USA). DMEM medium,Fetal Bovine Serum and Horse Serum were purchased from Thermo Fisher Scientific Inc. (Waltham, MA, USA). Amyloid-beta (1–42) Peptide and Donepezil were purchased from CAYMAN CHEMICAL COMPANY (Ann Arbor, Mich, USA). The medicine atorvastatin was purchased from Echo Chemical Co. Ltd. (Taiwan). Anti-beta Actin antibody,Anti-COX2/Cyclooxygenase 2 antibody,Anti-BDNF antibody, Goat Anti-Mouse IgG H&L (HRP) and Goat Anti-Rabbit IgG H&L (HRP) were purchased from abcam (Cambridge,UK). Anti-Caspase 3 antibodies were purchased from Proteintech Group Inc. (Chicago,IL,USA). ELISA MAX™ Deluxe Set Mouse TNF-α, ELISA MAX™ Deluxe Set Mouse IL-6, and ELISA MAX™ Deluxe Set Rat TNF-α were purchased from BioLegend (San Diego, CA,USA). Griess Reagent Kit was purchased from Biotium (San Francisco Bay Area, CA, USA).

2.3. OA extracts preparation

OA hot water extract (HW): Mixed 100 g of OA with 1 L of RO water,

and heated the water to 60 °C, shaken, and extracted for 24 h. Then the extract was filtered through a cloth funnel, and then a vacuum concentrator was used to concentrate the liquid and freeze-dried it. The 50% methanol extract (ME): Mixed 100 g of OA with 1 L of 50% methanol, shaken, and extracted at room temperature for 24 h. Filtered into a bucket, the liquid was concentrated by a vacuum concentrator and then freeze-dried. OA Chloroform Extract (CH): We mixed 100 g of OA grass with 1 L of chloroform, shaken, and extracted at room temperature for 24 h, and filtered it using a cloth funnel. The liquid was then concentrated to complete dryness with a vacuum concentrator. Methanol/ethyl acetate extraction of Aqueous Extract (ME/W): 100 g of OA was mixed with 1 L of 50% methanol, shaken, and then extracted at room temperature for 24 h. The liquid was filtered with funnel, then concentrated with a vacuum concentrator and an equal volume of ethyl acetate to added. It was placed it in a separatory funnel and left to stand until the layers were separated. The liquid of the ethyl acetate layer was collected, and concentrated to complete dryness by a vacuum concentrator. After methanol/ethyl acetate extraction, the remaining aqueous layer liquid was collected and concentrated under reduced pressure freeze-drying.

2.4. Determination of flavonoids and polyphenols levels in various OA extracts

Flavonoid content was determined using an aluminum chloride assay. Briefly, an aliquot (0.5 mL) of the extract was added to a 10 mL test tube containing 2 mL of distilled water. To each test tube, 0.3 mL of 5% $NaNO_2$ was added. After 6 min of incubation, 0.6 mL 10% $AlCl_3$ was added. After 1 min, 2 mL of 4% NaOH was added, and the volume was adjusted to 5 mL with distilled water. After 10 min, the absorbance of the resulting solution was measured at 510 nm. Quercetin was used as a standard to express the total flavonoid contents of samples as mg Quercetin equivalent per 100 g of sample (mg CE/100 g sample). All the samples were analyzed in triplicate.

Total phenolic concentration in the root extract was spectrophotometrically determined by the Folin–Ciocalteu assay, using gallic acid as a standard. The reaction mixture was prepared by mixing 0.5 mL of OA extract, 5 mL of distilled water, and 10 μL of 50% Folin-Ciocalteu reagent and shaken. After 5 min in the dark, 1 mL of 7.5% Na_2CO_3 was added and incubated at room temperature for 90 min in the dark. The reagent blank was also parallelly prepared using distilled water. The absorbance was measured against the prepared reagent blank at 510 nm using a double-beam UV/Vis spectrophotometer. The concentration of total phenolic compounds in the extract was expressed as milligrams of gallic acid equivalent (GAE) per 100 g sample (mg GAE/100 g) (Supplementary Table 1). All the samples were analyzed in triplicate.

2.5. Cell culture

The Mouse microglial cell line BV2 (ATCC® CRL-2467™) was purchased from American Type Culture Collection (Manassas, Va, USA). The cells were maintained in 90% DMEM medium, containing 10 mM HEPES, 1 mmol/L sodium pyruvate supplemented with 10% heat-inactivated fetal bovine serum, 1% penicillin-streptomycin, 2 mmol/L L-glutamine and pyridoxine hydrochloride. For experiments, the cells were subcultured in microtiter plates in the above culture medium and maintained in an incubator (95% air and 5% CO_2 at 37 °C, 90% humidity), and the medium was changed every 2 days until analysis.

The rat glioma cell line C6 (ATCC® CCL-107™) was purchased from the Food Industry Research and Development Institute (Taiwan). The cells were maintained in 82.5% Ham's F-10 medium, containing 2.5% heat-inactivated fetal bovine serum, 15% Horse Serum,1.5 g/L sodium bicarbonate, and 2 mmol/L L-glutamine. For further experiments, the cells were subcultured in microtiter plates in the above culture medium in an incubator (95% air and 5% CO_2 at 37 °C, 90% humidity), and the medium was changed every 2 days until analysis.

2.6. BV2 and C6 cell cytotoxicity

When the growth density of BV2 and C6 in the T75-flask reached 80–90%, after washing with PBS, trypsin was added to interact with the cells. After the cells were dispersed, the number of cells was counted with a hemocytometer, and an appropriate number of cells were cultured in a 96-well plate of 10% DMEM. Ham's F-10 was added in 100 μl of culture medium containing 10% FBS per well. After culturing for 24 h, when the cells adhered to the bottom, the culture medium was discarded. All the OA extracts were then added to the fresh culture medium for 24 h. Then 20 μl MTT solution (dissolved in 5 mg/mL PBS) was added to culture and put into a carbon dioxide incubator with 5% CO_2, 37 °C and a constant temperature of 90% humidity to react with the cells for 4 h. Thereafter, the solution was poured off from each well, and 100 μl DMSO added to each well to dissolve. Blue-violet crystals appeared, which was protected from light for about 10 min, and shaken the 96-well plates evenly to ensure blue-violet. The color crystals were completely dissolved, and the absorbance value at the wavelength of 570 nm was obtained by an enzyme immunoassay reader. As only living cells have active mitochondrial dehydrogenase, the measured light absorbance is proportional to the cell viability.

2.7. OA extracts protect BV2 and C6 from cellular injury pretreatment with $A\beta_{1\text{-}42}$

The viability of BV2 and C6 cells was measured by the reduction of MTT [3-(4,5-dimethylthiazol-2-yle) 2,5-mdiphenyltetralozium bromide]. Cells were harvested when in the exponential growth phase, cultured in 100 μL of fresh medium at 1×10^5 cells/well in 96-well plates. Cells were incubated in 5% CO2 at 37 °C for 24 h. Thereafter, the BV2 and C6 cells were induced with 10 μM concentration of β-amyloid 1–42 ($A\beta_{1\text{-}42}$) (Cayman Chemical Company 1.800.364.9897) for 24 h,and treated with d.d.H2O, Atorvastatin (10 μM), HW, ME, CH and ME/W *Orthosiphon aristatus* extract (0.01 mg/mL and 0.03 mg/mL) for 24 h, respectively. The reaction was continued for 24 h to estimate the cell viability. Cell proliferation was then assayed using the MTT assay in which PBS solution (20 μL) containing 5 mg/mL MTT was added to each well. Cells were further incubated for 4 h and then solubilized in 100 μL DMSO for optical density measurements at 570 nm. Cell survival was expressed as the ratio of the number of MTT-treated cells to the number of control cells (% of control).

2.8. RNA isolation and real-time PCR analysis

The RNA of BV2 and C6 from cells was isolated using a Phenol-Free Total RNA Purification Kit (Solon, IA, USA), and cDNA was synthesized using an iScript reverse transcriptase kit (Bio-Rad Laboratories, Hercules, CA, USA). Real-time PCR was performed using the Applied Biosystems® 7500 Real-Time PCR Systems (Thermo Fisher Scientific Inc.). The resulting cDNAs were used to assay gene expression via real-time PCR using the following primers: (BV2 cell) GAPDH (Plus: 5′-GAG CTA CGT GCA CCC GTA AA-3′/Minus: 5′-CAA AAA TGA GGC GGG TCC AA-3′); IL-6 (Plus: 5′-CCT CTG GCG GAG CTA TTG AG-3′/Minus: 5′-AGC ATC AGT CCC AAG AAG GC-3′); TNF-α(Plus:5′-CGC GGA TCA TGC TTT CTG TG-3′/Minus: 5′-GGA CTA GCC AGG AGG GAG AA-3′); NFκB (Plus: 5′-AGG GCA TGT GTC AAT TGG GT-3′/Minus: 5′-CAA AGG TCT GCC CAC CTC C-3′. (C6 cell) GAPDH (Plus: 5′-AGC CCA GAA CAT CAT CCC TG-3′/Minus: 5′-CAC CAC CTT CTT GAT GTC ATC-3′); IL-6 (Plus: 5′-CTG CTC TGG TCT TCT GGA GT-3′/Minus: 5′-GCA TTG GAA GTT GGG GTA GG-3′); iNOS (Plus:5′-CAC ACA GCC TCA GAG TCC TT-3′/Minus: 5′-CAG GGC TCG ATC TGG TAG TA-3′); IL-1β (Plus: 5′-CAC CTC TCA AGC AGA GCA CAG-3′/Minus: 5′-GGG TTC CAT GGT GAA GTC AAC-3′); TNF-α (Plus:5′-CTG AAC TTC GGG GTG ATC GG-3′/Minus: 5′-GGC TTG TCA CTC GAG TTT TGA GA-3′). All reactions were made using qPCR™ Core Kit for SYBR Green I®, the most frequently used dsDNA specific dye Data analysis using the $2^{-\Delta\Delta Ct}$ method and its validation. Each experiment

was performed in triplicate.

2.9. Western blot analysis-based determination of cellular protein level

At the end of the experiment, all mice were sacrificed, and their livers prepared for the analysis of expression of proteins relevant to insulin resistance. The tissues were ground, centrifuged, and incubated in protein extraction buffer for 1 h. Samples were centrifuged at 14,000 rpm for 30 min. Proteins were separated by 10% PAGE, then transferred onto nitrocellulose membranes. After blocking, membranes were incubated with anti-COX-2 antibody and anti-BDNF antibody (1:200) for 1 h at room temperature in rinse buffer, followed by four washes of 10 min each. Horseradish peroxidase-conjugated anti-rabbit IgG and anti-mouse IgG antibodies was diluted 1: 5000 in rinse buffer and incubated with blots for 1 h at room temperature. Horseradish peroxidase was added (Reagent A + Reagent B, 1:1 ratio) to visualize antibody-bound COX-2 and BDNF protein on the NC membrane. Western blot images were obtained using a LAS-3000 analyzer (Fuji, Japan).

2.10. Animals preparation

Male ICR mice at 8 weeks of age (age 9 weeks at the time of injury) were purchased from the National Laboratory Animal Center (Taiwan). All animals were maintained in laminar flow cabinets with free access to food and water under specific pathogen-free conditions in facilities. The mice acclimatized to 12:12 h light-dark cycle conditions in the cages. Animals were kept in a housing facility for a 1-week acclimation period before the surgical injury and were kept in a housing facility for 2-week acclimation period before $A\beta_{1-42}$ is infused into mice's brains to mimic Alzheimer's disease.

The mice were fed with d.d. H_2O, Atorvastatin, HW, ME, CH, and ME/W for 14 days. Then, all subject mice were anesthetized by intraperitoneal injection of sodium pentobarbital (50 mg/kg) and then placed on the animal stereotaxic apparatus to locate the left lateral ventricle. Considering bregma on the cranial bones as the center, that lateral ventricle was localized and drilled at the position of 0.4 mm vertical axis and 1.0 mm horizontal axis. $A\beta_{1-42}$ Oligomer (400 pmol) in 35% Acetonitrile/0.1% Trifluoroacetic Acid (pH 2.0) solution was injected with 5 μl Hamilton Microsyringe I.C.V. into the Bilateral ventricular regions into a depth of 2.0 mm from the cranial bones. Fixed the gasket on the cranial bones with bioadhesive, and finally sutured with a sewing needle. The mice were kept in a 37 °C room for several hours to prevent hypothermia and then returned to the rearing cage for care. Further, animal behavioral experiments were started after they returned to their normal activities (about 5 days).

2.11. Group experimental designs in mice

All mice were randomized into 6 groups (n = 6): (1) Control, (2) Sham: without $A\beta_{1-42}$ treatment; (3) $A\beta_{1-42}$: animals were given intragastrically with a single dose of intracerebroventricular injection of $A\beta_{1-42}$ (5 μM); (4) Donepezil + $A\beta_{1-42}$: animals intragastrically administered with a single dose of donepezil (3 mg/kg) followed by intracerebroventricular injection of $A\beta_{1-42}$ (5 μM) (5) ME/W 100 mg/kg + $A\beta_{1-42}$: animals intragastrically with a single dose of OA (100 mg/kg) obtained through *aqueous extract of ethyl acetate extraction* (100 mg/mL) followed by intracerebroventricular injection of $A\beta_{1-42}$ (5 μM). (6) ME/W 300 mg/kg + $A\beta_{1-42}$: animals intragastrically with a single dose of OA (300 mg/kg) obtained through *aqueous extract of ethyl acetate extraction* followed by intracerebroventricular injection of $A\beta_{1-42}$ (5 μM).

2.12. Passive avoidance test (PAT)

PAT to assess long-term memory and emotional learning towards aversive stimuli was conducted in line with previous studies (Liu et al., 2022; Van Dam et al., 2008). The composition of the PAT equipment is an aluminum shuttle cage of 72 (length) × 34 (width) × 24 (height) cm^3 (Coulbourn Instruments Model E10-15), divided into a bright room and a dark room. It includes a guillotine door (Coulbourn Instruments Model E10-15GD) of 7.5 (L) × 6.5 (W) cm^2 in the center, and the bottom of the shuttle cage is set with metal rods arranged in parallel with an interval of 1 cm, connect the current device. First, the mice were placed in a bright room, and after 10 s of adaptation, the small gate of the septum was opened to allow them to explore freely. Once the mice entered the dark room, the small gate was quickly closed and conducted low-voltage 33 V with a 5-s electric shock to the mice's feet. It lasts 5 s for one electric shock, three times in total, and the learning training was completed. After 24 h, the animal was placed in the bright room, and the gate was opened at the same time, step-through latency of the animal in the bright room was recorded. The longer the latency time in the bright room, the better the learning training and memory ability. In this experiment, the infrared rapid scanning detection system in the Shuttle Avoidance Instrument was used to accurately and timely measure the shuttle times and latency of mice. The maximum duration of each test is 180 s.

2.13. Spatial tracking in the Morris water maze (MWM)

The MWM, as a behavioral test used to *assess spatial learning and memory*, was conducted in accordance with previous studies (Van Dam et al., 2008). The Reference Memory Task is one of the evaluation methods of the Hidden-Platform Acquisition Train, which is mainly used to measure the learning and memory ability of animals in the water maze (an evaluation method of long-term memory ability), the experiment lasted for 4 days. The diameter of the circular swimming pool is 140 cm, and the height is 45 cm. The swimming pool has a diameter of 12 cm and a height of 25 cm movable rest platform. Before the experiment, the swimming pool must be filled with water to 27 cm level height. The pool area is divided into four quadrants (I, II, III, and IV), and 5 starting points are set. The resting platform is kept at the center point of any quadrant. Half an hour before the experiment, the mice were placed in the room where the water maze was located to adapt to the environment. Each mouse was trained twice daily, the resting platform was fixed on one of the quadrants, and the animals headed outwards and randomly entered the four entry points. During the experiment, a camera was set up above the central point of the swimming pool to record the swimming path and latency of the experimental mice in each quadrant. Further statistical analysis (Animal Video Behavior System) was performed on the time/path length, average movement speed, times of passing through the virtual platform, and latency time on the virtual platform of the experimental mice in a specific area. The maximum duration of each test is 180 s.

2.14. Statistical analysis

SigmaPlot 14.0 software was used for experimental data processing and drawing. The statistical representation of experimental results was mean ± standard error (mean ± S.E.). *In vitro* experiments, the P value of the difference between groups was calculated using *t-test* in SigmaPlot software. *In vivo* experiments, sample differences were computed using ONE-WAY ANOVA plus a post-hoc test (Scheffe method) to calculate the P value. P values less than 0.05 were considered statistically significant. Western Blot and RT-PCR used Image J as the basis for quantification, and SigmaPlot 14.0 was used for statistical analysis after completion.

3. Results

3.1. Impact of OA on $A\beta_{1-42}$ induced cytotoxicity

We conducted the MTT assay to assess the impact of different OA extracts on $A\beta_{1-42}$-induced toxicity in BV2 cells. It was observed that compared to atorvastatin, CH, and ME/W extracts at 0.01 mg/mL and

0.03 mg/mL were more effective in improving cell viability (Fig. 1A). Additionally, CH extract at 0.01 mg/mL was the most effective candidate against $A\beta_{1-42}$ (10 μM)-induced cytotoxicity. Further, atorvastatin, ME extract at 0.01 and 0.03 mg/mL and CH extract at 0.03 mg/mL were equally effective. Notably, ME/W extract at 0.01 mg/mL was more toxic to C6 cells than atorvastatin (Fig. 1B).

Neuroinflammation influences the neuronal population in the central nervous system (Lau, 2009). Remarkably, nuclear factor-κB (NF-κB) is involved in the regulation of inflammation and plays a crucial role in amyloidogenesis, leading to the development of AD (Ju Hwang et al., 2019; Liu et al., 2017; Oeckinghaus and Ghosh, 2009). Therefore, in this study, we used the $A\beta_{1-42}$-induced BV2 microglia cell line to investigate the neuroprotective effects of OA extracts. We specifically aimed to check whether OA exerts any effects on BV2 cells by regulating inflammatory molecules such as IL-6, TNF-α, and NF-κB. Our ELISA results demonstrated that compared to atorvastatin (10 μM), and CH extract of OA at 0.03 mg/mL significantly lowered the expression of IL-6, TNF-α, and NF-κB, in BV2 cell line (Fig. 2A–C). Similarly, the potential of OA extracts in regulating the expression of IL-6, NF-κB, and iNOS mRNA was also evaluated in C6 cells. Of note, our results showed that ME/W extract at 0.03 mg/mL was most effective ($p < 0.05$) in downregulating the expression of IL-6, NF-κB, and iNOS in comparison to atorvastatin (10 μM) and other extracts (Fig. 2D–F). In addition, HW extract compared to atorvastatin (10 μM), was significantly effective in downregulating the expression of IL-6, and NF-κB.

3.2. OA extract on COX-2 and BDNF protein levels

Cyclooxygenase (COX)-2 is an inflammatory molecule involved in the progression of neurodegenerative disorders (Minghetti, 2004). To measure the effect of different OA extracts on COX-2 protein level in the $A\beta_{1-42}$-induced BV2 cell line is observed. We found that COX-2 level was significantly increased in BV2 cells after challenge with $A\beta_{1-42}$. Notably, in comparison to atorvastatin (10 μM), the COX-2 level was significantly high among all groups of OA extracts (Fig. 3A). Notably, among all OA extracts, ME/W extract at 0.03 mg/mL was most effective in reducing the level of COX-2 protein level.

Brain-derived neurotrophic factor (BDNF) as an oncogenic factor contributes significantly to the initiation and progression of tumors (Yang et al., 2017). BDNF also plays a crucial role in the growth and apoptosis of the glioma C6 cell line. To determine the impact of OA extracts on BDNF protein level, we measured the BDNF level by western blotting. Our results indicate that BDNF levels significantly lowered in C6 cells due to exposure to $A\beta_{1-42}$. Notably, in comparison to atorvastatin (10 μM), ME of OA among other extracts at 0.03 mg/mL was most effective ($p < 0.05$) in increasing the BDNF level (Fig. 3B). However, ME/W at 0.03 mg/mL reported the lowest increase in BDNF level in comparison to atorvastatin (10 μM) and other OA extracts.

3.3. Effect of OA on spatial memory and learning

3.3.1. Passive avoidance test (PAT)

To determine the avoidance memory retention (AMR) in mice, the PAT was performed. The mice were placed in an aluminum shuttle cage containing a bright room and a dark room with a guillotine door. We utilized donepezil to assess its impact on animal behavior, primarily focusing on AD-related pathologies, particularly its effects on cognition and memory functions. Donepezil is a type of acetylcholinesterase inhibitor that especially enhances cholinergic neurotransmission in the brain to improve cognitive functions (Grossberg, 2003). Our results demonstrated that $A\beta_{1-42}$ exposure to experimental mice significantly lowered the AMR. However, the ME/W extract of OA at 100 mg/kg showed comparable improvement in avoidance memory retention to donepezil at 3 mg/kg on day 5 (Fig. 4). Remarkably, the ME/W extract of OA at 300 mg/kg was most effective in improving AMR.

3.3.2. Effect of OA extract in Morris water maze (MWM) test

To determine the effect of OA extracts on spatial memory and learning, the MWM behavior test was performed. Test mice were injected with $A\beta_{1-42}$ (410 pmol/5 μl), saline, donepezil (3 mg/kg), and ME/W extracts at 100 mg/kg and 300 mg/kg. Notably, donepezil (3 mg/kg) and ME/W extracts at 300 mg/kg showed comparable improvement in finding hidden platforms (Fig. 5A). Further, the ME/W extract at 100 mg/kg also showed significant improvement in the performance of test mice; however, the effect was less than donepezil and ME/W extracts at 300 mg/kg.

3.3.3. Effect of OA extract on escape latency

The MWM test further demonstrated that injection of $A\beta_{1-42}$ in mice significantly deteriorates spatial memory and learning, as indicated by the remarkably high escape latency. However, MW/E extracts at 100 mg/kg and 300 mg/kg showed a significant reduction in escape latency compared to donepezil (3 mg/kg) (Fig. 5B). Notably, ME/W extract at 300 mg/kg resulted in the lowest escape latency period compared to donepezil and MW/E extracts at 100 mg/kg.

4. Discussion

The increasing prevalence of neurodegenerative disorders such as AD will be approximately triple that of cognitive impairment and dementia patients by 2050 (Mat Nuri et al., 2017; Retinasamy et al., 2019; Scheltens et al., 2021a,b). Notably, β-amyloid peptide, in particular $A\beta_{1-42}$, and NFTs are the major cause of cognitive and memory loss due to β-amyloid toxicity and NFTs-mediated neuronal loss (Kopeikina et al.,

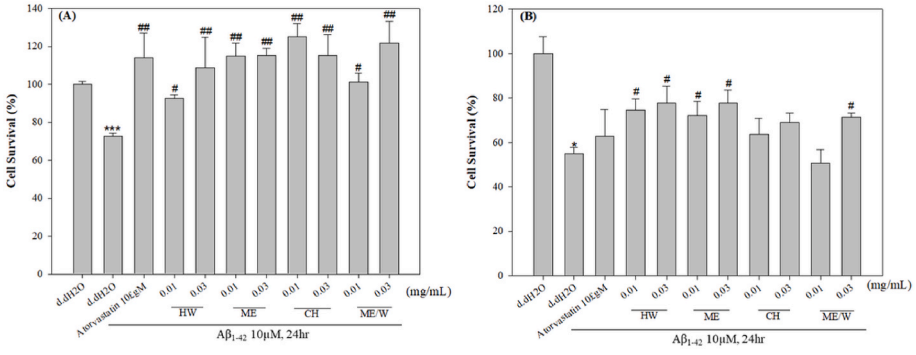

Fig. 1. Effect of OA extracts on cell survival of (A) BV2 cells and (B) C6 cells. The cells were first administered $A\beta_{1-42}$ 10 μM for 24 h to induce injury, followed by atorvastatin (10 μM) and 0.01 mg/mL, 0.03 mg/mL, 0.1 mg/mL of each group of OA extracts, and MTT assay was conducted after 24 h. Data are expressed as mean ± SE (n = 3). *$p < 0.05$ compared with the control group. $^{\#}p < 0.05$, and $^{\#\#}p < 0.01$ compared with ddH_2O group. OA, *Orthosiphon aristatus*; d.d H_2O, double distilled water; HW, Hard water extract; ME, methanol extract; CH, Chloroform extract, ME/W, Methanol/water extract of *Orthosiphon aristatus*.

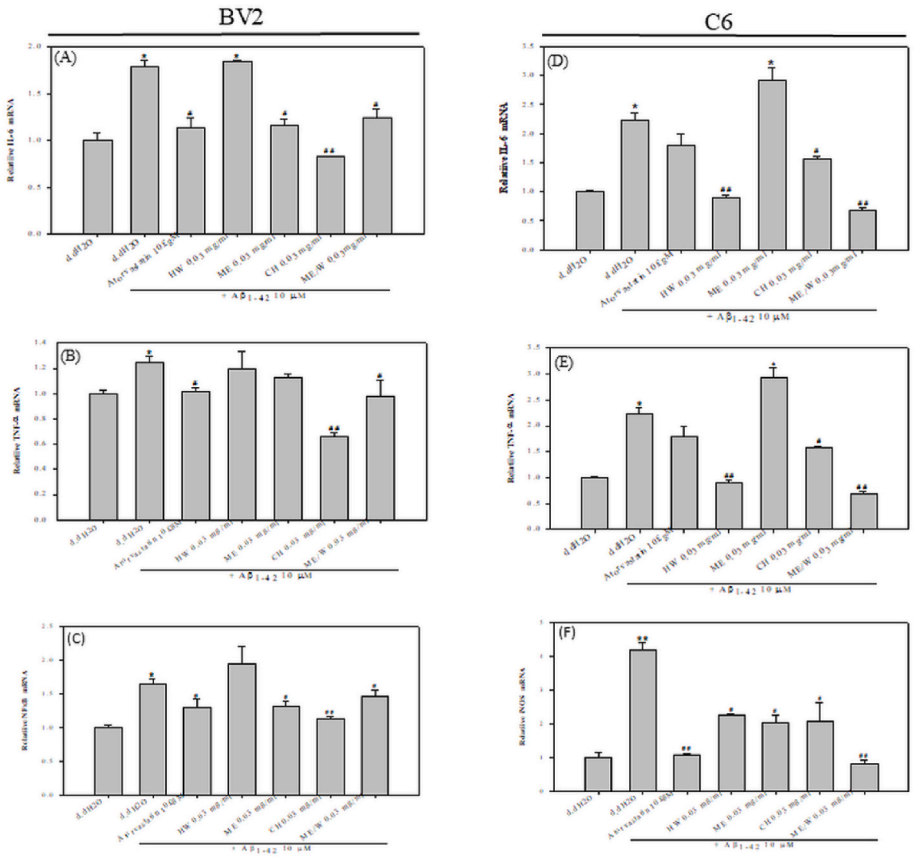

Fig. 2. Effect of OA extracts on the mRNA expression levels of (A) IL-6, (B) TNF-α, and (C) NF-κB in BV2 cells. Further, the mRNA expression levels of (D) IL-6, (E) NF-κB, and (F) iNOS were also examined in C6 cells. OA, *Orthosiphon aristatus*; d.d H_20, double distilled water; HW, Hard water extract; ME, methanol extract; CH, Chloroform extract, ME/W, Methanol/water extract of *Orthosiphon aristatus.* Data are expressed as mean ± SE (n = 3). *$p < 0.05$ compared with the control group. $^{\#}p < 0.05$, $^{\#\#}p < 0.01$ compared with ddH_2O group.

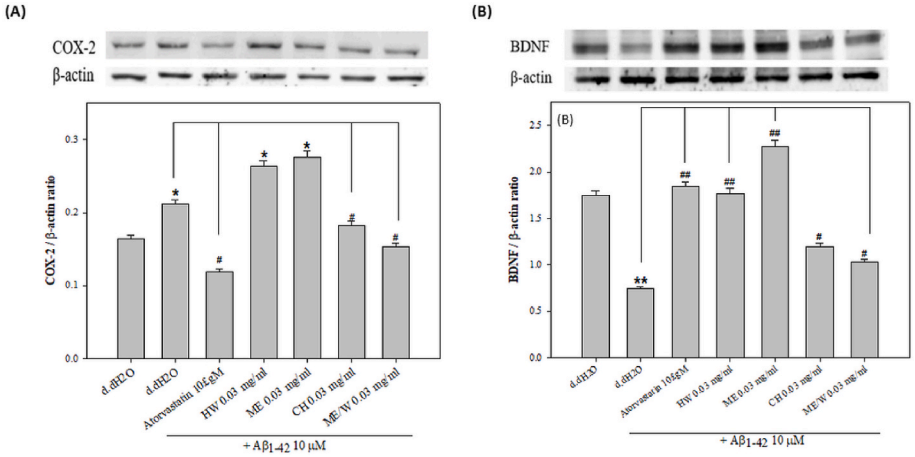

Fig. 3. The inhibitory effect of OA extracts on the protein expression levels of (A) COX-2 protein in BV2 cells and (B) BDNF in C6 cells. Data are expressed as mean ± SE (n = 3). **$p < 0.01$, ***$p < 0.001$ compared with control group. $^{\#}p < 0.05$, $^{\#\#}p < 0.01$, $^{\#\#\#}p < 0.001$ compared to ddH2O group. OA, *Orthosiphon aristatus*; d. d H20, double distilled water; HW, Hard water extract; ME, methanol extract; CH, Chloroform extract, ME/W, Methanol/water extract of *Orthosiphon aristatus.*

2012; Retinasamy et al., 2019). Current pharmaceutical agents such as cholinesterase inhibitors and partial NMDA receptor antagonists are the only effective alternatives for partial symptomatic relief (Obulesu and Rao, 2011; Retinasamy et al., 2019). Traditional Chinese medicines are rich sources of therapeutic constituents, some of which are potent anti-oxidative agents and could play an effective role in the treatment of neurodegenerative disorders (Mahdy et al., 2012; Retinasamy et al., 2019; Silva et al., 2005). Based on this evidence, we evaluated the therapeutic potential of various OA extracts *in-vivo* and *in-vitro.*

To determine the impact of OA extracts on $A\beta_{1\text{-}42}$ induced toxicity on BV2 and C6 cells, MTT assays were performed. Our results indicate that CH and ME/W extracts at 0.03 mg/mL OA concentration significantly improved cell survival compared to atorvastatin (10 μM). Further, it indicated that both OA extracts are most effective in reducing the $A\beta_{1\text{-}42}$

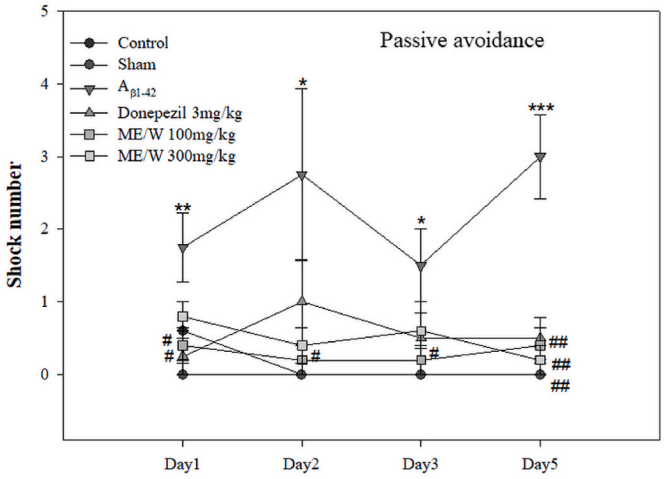

Fig. 4. Passive avoidance test in mice after administration of test substances. The induced mice were randomly divided into groups and administered Saline, Donepezil 3 mg/kg, ME/EA 100 mg/kg, ME/EA 300 mg/kg, the passive avoidance test was performed after 14 days of continuous administration of the test substance. Each trial time was 5 min. The total number of times that mouse entered the dark room was recorded. Data are expressed as mean ± SE (n = 4). *p < 0.05, **p < 0.01, ***p < 0.001 compared with sham group. #p < 0.05, ##p < 0.01 compared with saline group.

induced cytotoxicity on BV2 cells. Notably, all OA extracts at 0.01 and 0.03 mg/mL concentrations were found effective in protecting BV2 cells against $A\beta_{1\text{-}42}$ cytotoxicity. Notably, similar to our results, Retinasamy et al. found that the ethanolic extract of *Orthosiphon stamineus* (OS) was effective in reducing the effect of β-amyloid toxicity on SH-SY5Y human neuroblastoma cells (Retinasamy, 2019). The study indicates that OS and Rosmarinic acid mediate their effect by inhibiting the enzymatic activity of Acetylcholinesterase (AChE). Moreover, the ethanolic extract of OS promotes the growth of immature neurons in the hippocampal region and significantly reverses the suppression of adult neurogenesis (Retinasamy et al., 2019). In addition, ethanolic extracts of OA also lowered the LPS-induced oxidative stress and inflammatory stress on BV2 cells by radical scavenging and inhibiting NO production (Hwang et al., 2021). We further evaluated the effect of OA extracts on $A\beta_{1\text{-}42}$-induced C6 cells. Our finding reports that HW and ME extract of OA at 0.01 mg/mL concentration were most effective in improving C6 cell survival. In addition, all extracts except ME/W at 0.01 mg/mL concertation showed increased cell survival compared to atorvastatin. It could be inferred that OA extracts are also effective in lowering the toxic effect of the amyloid peptide on C6, a rat glioma cell line. However, in contrast to our study, another study indicated that the extracts of *Orthosiphon stamineus* Benth have significantly reduced the level of nucleolin and bcl-2 expression in MCF-7 cells, resulting in a significant decrease in the MCF-7 cell population (Saravanan et al., 2017). A similar effect of high cytotoxic effect of OS was observed on T47D breast cancer cells line, and the anticancer properties were associated with sinensetin (Arifianti et al., 2020). In addition, purified OA-derived sinensetin arrested cell growth of hepatocellular carcinoma cells (HCC) at G0/G1 phase and downregulated Bcl-xL along with upregulation of tumor suppressor TRAIL and PTEN, resulting in a cytotoxic effect on HCC (Samidurai et al., 2020). Conclusively, these studies are in contrast to our study. However, our study demonstrates that OA is also efficient in mitigating the toxic effect of $A\beta_{1\text{-}42}$ on the C6 glioma cell line.

The effect of OA extract on the expression of pro-inflammatory molecules such as IL-6, TNF-α, and NF-κB in $A\beta_{1\text{-}42}$ induced BV2 cells has also been examined. Our results demonstrate that the CH extract of OA is the most effective in significantly lowering the expression of cytokines and inflammatory molecules i.e., IL-6, TNF-α, and NF-κB compared to atorvastatin (10 μM). Similar to our results, Hsu et al. also reported that ethanol extracts of OA and its bioactive molecule ursolic acid significantly lower the oxidative stress in LPS-induced RAW264.7 cells by downregulating the expression of iNOS and COX-2, resulting in suppression of induced nitric oxide (NO) and prostaglandin E2 (PGE2) (Hsu et al., 2010). The cumulative effect of these changes results in suppressing reactive oxygen species (ROS). Likewise, the ethanolic extracts of OS significantly inhibit the production of TNF-α, IL-1 COX-1, and COX-2 in the LPS-induced U937 macrophages (Tabana et al., 2016). The OS extract has also improved joint integrity, protected cartilage and soft tissue, and recovered tibia-talus bones from osteoporotic lesions in rat models. These findings indicate OS's potential in treating rheumatoid arthritis and other inflammatory disorders. Notably, the antioxidant metabolites such as polyhydrolic alcohols, trihydroxy-octadecenoic acid, oxo-dihydroxy-octadecenoic acid, and 9-oxo-octadecadienoic acid of OA also contribute to its antioxidation potential (Wahab and Chua, 2022). Our finding also suggests that ME/W extracts at 0.03 mg/mL concentration significantly lower the expression of IL-6, NF-κB, and iNOS in C6 cells. The ethanolic extract of OS in combination with gemcitabine has also been found effective in lowering the expression of multidrug-resistant (MDR) protein family, epithelial-mesenchymal transition molecules such as ZEB-1 and Snail-1, suppression of Notch intracellular domain, and inducing the expression of human equilibrate nucleoside transporter-1 (hENT-1) gene. These molecular changes promotes cellular senescence, cell cycle arrest, and cell death resulting in

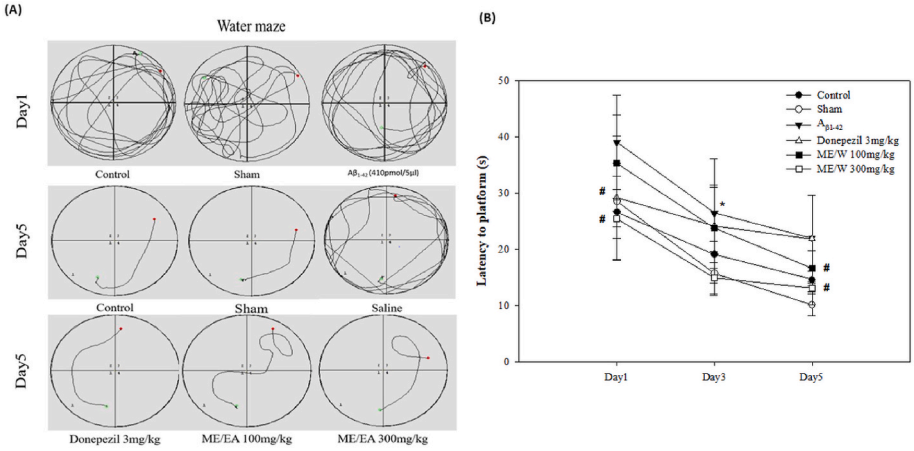

Fig. 5. Determination of time to reach the hidden platform in the Morris water maze test. The induced mice were randomly divided into groups and administered with Saline, Donepezil 3 mg/kg, ME/EA 100 mg/kg, ME/EA 300 mg/kg, the water maze test was performed after 14 days of continuous administration of the test substances. Data are expressed as mean ± SE (n = 4). *p < 0.05 compared with sham group.

inhibition of growth of pancreatic cancer cell line (Panc-1) (Yehya et al., 2021). However, the combination of gemcitabine and rosmarinic acid was not effective in demonstrating any significant effect on apoptosis, cellular senescence, epithelial-mesenchymal transition (EMT) markers, hENT-1, Notch pathway, and the MRP-4 and MRP-5 multi-drug resistance protein family. The NO inhibitory activity of OS could be associated with concentration gradients of diterpenes (Abdullah et al., 2020; Awale et al., 2003). The downregulation of NO reduces the secretion of pro-inflammatory cytokines such as interleukin-1 (IL-1), tumor necrosis factor, and interferon (Abdullah et al., 2020; Kuo and Schroeder, 1995). The optimized supercritical CO_2 extracts of OS (B2) effectively demonstrated its cytotoxic and anti-oxidative impact on prostate cancer (PC3) cells, though no toxic effect was observed on the normal human colonic fibroblast (CCD-18Co) cells (Al-Suede et al., 2014).

We have further evaluated the effect of OA extracts on COX-2 and BDNF protein expression in BV2 and C6 cells, respectively. Our results demonstrate that ME/W extract at 0.03 mg/mL is most effective in significantly lowering the level of COX-2 and BDNF compared to atorvastatin (10 μM). Notably, LPS stimulation could induce neuroinflammation by activating microglial cells and results in overexpression of the COX-2 in BV2 cells, which further increases the level of inflammatory cytokines such as IL-6 by activating Stat3 signaling pathway along with other cytokines IL-1β, TNF-α, and MCP-1 (Al-Suede et al., 2014). Similar to our study, Torilin isolated from the Stem and root bark of *Ulmus davidiana* var. *japonica* (Ulmaceae) could significantly lower the level of inflammatory cytokines such as iNOS, COX-2 and IL-1β by inhibiting the activation of extracellular signal-regulated kinase 1/2 (ERK1/2) and p38 MAPK in LPS-induced BV2 cell lines (Choi et al., 2009). Similar to our results, Hsu et al. reported that alcoholic OA extracts effectively lower the COX-2 and iNOS mRNA levels in RAW264.7 Cells (Hsu et al., 2010). In addition, epigallocatechin gallate (EGCG), an active component of green tea, also demonstrates its antioxidant and anti-inflammatory properties by inhibiting the NF-κB pathway, suppressing hypoxia-inducible factor (HIF)-1α, and ROS generation in BV2 Cells (Kim et al., 2022). The EGCG also downregulates the secretion of inflammatory molecules such as IL-6, iNOS, and COX-2.

Similarly, the ME/W at 0.03 mg/mL concentration effectively lowers the BDNF level in the C6 cell. BDNF, a neurotrophic factor, is crucial in promoting cell growth, survival, proliferation, and migration of cancerous cells and is overexpressed in cancer related to the breast, lung, prostate, and underlying tissues (Malekan et al., 2022). Thus, the downregulation of BDNF in cancer cells could also be a practical approach to provide therapeutic relief. Notably, OS or OA modulates BDNF-TrkB and CREB-BDNF signaling pathways along with neurogenesis, which results in the impediment of cognitive and memory impairment (Chung et al., 2020c; Toledo and Inestrosa, 2010).

We have performed PAT and MWM tests to evaluate the effect of OA extracts on spatial and learning memory. The result of PAT reported that ME/W extract at 300 mg/kg can significantly improve the performance. Similar to our results, in the rat model, the ethanolic extract of OS at 50, 100, and 200 mg/kg has significantly elevated step-through latency, indicating an improvement in memory retention (Retinasamy et al., 2020). Furthermore, our MWM test demonstrates that ME/W extract at 300 mg/kg is most effective in improving performance to reach the hidden platform and escape latency compared to atorvastatin and other OA extracts under study. Notably, in line with our results, Retinasamy et al. reported that ethanolic extract of OA efficiently decreased escape latency in the MWM test (Retinasamy, 2019). The ethanolic extract of OS effectiveness in improving spatial and memory learning has been associated with its potential to inhibit adenosine A_1 receptor (A1R) and A_{2A} receptors (A2AR) activity, resulting in a decrease in neurodegeneration (George et al., 2015). Apart from several strengths like animal-based PAT and MWM tests revealing *in vivo* impacts, our study also includes a few limitations, such as a detailed mechanistic exploration related to the effect of OA.

5. Conclusion

Our study evaluated the potential of OA in treating βA_{1-42} toxicity-induced AD. Our findings indicate the potential of ME/W-OA extract, specifically at 300 mg/kg dose, which improved spatial learning and memory *in vivo,* possibly through significantly reducing inflammatory factors including TNF-α, IL-6, IL-1β, COX-2, and iNOS, and increasing BDNF levels. However, more wide-spectrum studies are required to establish the clinical potential of OA with detailed mechanistic insight.

Ethics statement

All animal experiments were conducted according to the Animal Care and Use Committee guidelines of the Southern Taiwan University of Science and Technology. The protocol was approved by the Institutional Animal Care and Use Committee (IACUC) of Southern Taiwan University of Science and Technology (Approval No. STUST-IACUC-108-07).

CRediT authorship contribution statement

Kuang-Hsing Chiang: conceived and designed the study, read and revised the article. Tain-Junn Cheng: contributed to the data analysis and wrote the manuscript. Wei-Chih Kan: contributed to the data analysis and wrote the manuscript. Hsien-Yi Wang: contributed to the data analysis, performed experiments. Jui-Chen Li: performed experiments. Yan-Ling Cai: contributed to the data analysis, performed experiments. Chia-Hui Cheng: contributed to the data analysis, performed experiments. Yi-Chien Liu: contributed to the data analysis, performed experiments. Chia-Yu Chang: contributed to the data analysis, performed experiments. Jiunn-Jye Chuu: contributed to the data analysis, revised manuscript, and supervised the study. All the authors have confirmed the final manuscript.

Funding

This research received no external funding.

Declaration of competing interest

The authors declare that they have no known competing financial interests or personal relationships that could have appeared to influence the work reported in this paper.

Data availability

Data will be made available on request.

Acknowledgments

None.

Appendix A. Supplementary data

Supplementary data to this article can be found online at https://doi.org/10.1016/j.jep.2023.117132.

Abbreviations

AD	Alzheimer's disease
Aβ	Beta-amyloid
NFT	neurofibrillary tangles
OA	Orthosiphon aristatus
HW	Hot water extract
ME	Methanol extract
CH	Chloroform extract

TNF-α	Tumor necrosis factor-α
IL-6	Interleukin-6
IL-1β	Interleukin-1β
COX-2	Cyclooxygenase
iNOS	Inducible nitric oxide synthase

References

Abdullah, F.I., Chua, L.S., Mohd Bohari, S.P., Sari, E., 2020. Rationale of orthosiphon aristatus for healing diabetic foot ulcer. Nat. Prod. Commun. 15 (9), 1934578X20953308.

Al-Suede, F.S.R., Khadeer Ahamed, M.B., Abdul Majid, A.S., Baharetha, H.M., Hassan, L. E.A., Kadir, M.O.A., Nassar, Z.D., Abdul Majid, A.M.S., 2014. Optimization of cat's whiskers tea (*Orthosiphon stamineus*) using supercritical carbon dioxide and selective chemotherapeutic potential against prostate cancer cells. Evid. Based Compl. Alternative Med. 2014, 396016.

Alshehade, S.A., Al Zarzour, R.H., Murugaiyah, V., Lim, S.Y.M., El-Refae, H.G., Alshawsh, M.A., 2022. Mechanism of action of Orthosiphon stamineus against non-alcoholic fatty liver disease: insights from systems pharmacology and molecular docking approaches. Saudi Pharm. J: Off. Publ. Saudi Pharm. Soc. 30 (11), 1572–1588.

Arifianti, L., Sukardiman, S., Indriyanti, N., Widyowati, R., 2020. Anticancer property of orthosiphon stamineus benth. Extracts in different solvent systems against t47d human breast cancer cell lines. Fabad J. Pharm. Sci. 45 (3), 187–194.

Ashrafian, H., Zadeh, E.H., Khan, R.H., 2021. Review on Alzheimer's disease: inhibition of amyloid beta and tau tangle formation. Int. J. Biol. Macromol. 167, 382–394.

Awale, S., Tezuka, Y., Banskota, A.H., Kadota, S., 2003. Inhibition of NO production by highly-oxygenated diterpenes of Orthosiphon stamineus and their structure–activity relationship. Biol. Pharm. Bull. 26 (4), 468–473.

Benseny-Cases, N., Klementieva, O., Cotte, M., Ferrer, I., Cladera, J., 2014. Microspectroscopy (μFTIR) reveals Co-localization of lipid oxidation and amyloid plaques in human alzheimer disease brains. Anal. Chem. 86 (24), 12047–12054.

Bloom, G.S., 2014. Amyloid-β and tau: the trigger and bullet in Alzheimer disease pathogenesis. JAMA Neurol. 71 (4), 505–508.

Breijyeh, Z., Karaman, R., 2020. Comprehensive review on Alzheimer's disease: causes and treatment. Molecules 25 (24), 5789.

Burke, S.L., Cadet, T., Alcide, A., O'Driscoll, J., Maramaldi, P., 2018. Psychosocial risk factors and Alzheimer's disease: the associative effect of depression, sleep disturbance, and anxiety. Aging Ment. Health 22 (12), 1577–1584.

Castegna, A., Aksenov, M., Aksenova, M., Thongboonkerd, V., Klein, J.B., Pierce, W.M., Booze, R., Markesbery, W.R., Butterfield, D.A., 2002. Proteomic identification of oxidatively modified proteins in alzheimer's disease brain. part I: creatine kinase BB, glutamine synthase, and ubiquitin carboxy-terminal hydrolase L-1. Free Radic. Biol. Med. 33 (4), 562–571.

Chatterjee, S., Peters, S.A., Woodward, M., Mejia Arango, S., Batty, G.D., Beckett, N., Beiser, A., Borenstein, A.R., Crane, P.K., Haan, M., 2016. Type 2 diabetes as a risk factor for dementia in women compared with men: a pooled analysis of 2.3 million people comprising more than 100,000 cases of dementia. Diabetes Care 39 (2), 300–307.

Chau, C.F., Wu, S.H., 2006. The development of regulations of Chinese herbal medicines for both medicinal and food uses. Trends Food Sci. Technol. 17 (6), 313–323.

Cheignon, C., Tomas, M., Bonnefont-Rousselot, D., Faller, P., Hureau, C., Collin, F., 2018. Oxidative stress and the amyloid beta peptide in Alzheimer's disease. Redox Biol. 14, 450–464.

Chen, G.F., Xu, T.H., Yan, Y., Zhou, Y.R., Jiang, Y., Melcher, K., Xu, H.E., 2017. Amyloid beta: structure, biology and structure-based therapeutic development. Acta Pharmacol. Sin. 38 (9), 1205–1235.

Choi, Y., Lee, M.K., Lim, S.Y., Sung, S.H., Kim, Y.C., 2009. Inhibition of inducible NO synthase, cyclooxygenase-2 and interleukin-1beta by torilin is mediated by mitogen-activated protein kinases in microglial BV2 cells. Br. J. Pharmacol. 156 (6), 933–940.

Chua, L.S., Lau, C.H., Chew, C.Y., Ismail, N.I.M., Soontorngun, N., 2018. Phytochemical profile of Orthosiphon aristatus extracts after storage: rosmarinic acid and other caffeic acid derivatives. Phytomedicine 39, 49–55.

Chung, Y.S., Choo, B.K.M., Ahmed, P.K., Othman, I., Shaikh, M.F., 2020a. *Orthosiphon stamineus* proteins alleviate pentylenetetrazol-induced seizures in Zebrafish. Biomedicines 8 (7), 191.

Chung, Y.-S., Choo, B.K.M., Ahmed, P.K., Othman, I., Shaikh, M.F., 2020b. A systematic review of the protective actions of cat's whiskers (Misai Kucing) on the central nervous system. Front. Pharmacol. 692.

Chung, Y.-S., Choo, B.K.M., Ahmed, P.K., Othman, I., Shaikh, M.F., 2020c. A systematic review of the protective actions of cat's whiskers (Misai Kucing) on the central nervous system. Front. Pharmacol. 11.

De Felice, F.G., Lourenco, M.V., 2015. Brain metabolic stress and neuroinflammation at the basis of cognitive impairment in Alzheimer's disease. Front. Aging Neurosci. 7, 94.

Ezeani, M., Omabe, M., 2016. A new perspective of lysosomal cation channel-dependent homeostasis in Alzheimer's disease. Mol. Neurobiol. 53 (3), 1672–1678.

Figueiro, M.G., Plitnick, B.A., Lok, A., Jones, G.E., Higgins, P., Hornick, T.R., Rea, M.S., 2014. Tailored lighting intervention improves measures of sleep, depression, and agitation in persons with Alzheimer's disease and related dementia living in long-term care facilities. Clin. Interv. Aging 9, 1527–1537.

Frozza, R.L., Lourenco, M.V., De Felice, F.G., 2018. Challenges for Alzheimer's disease therapy: insights from novel Mechanisms beyond memory defects. Front. Neurosci. 12, 37.

George, A., Chinnappan, S., Choudhary, Y., Choudhary, V.K., Bommu, P., Wong, H.J., 2015. Effects of a proprietary standardized *Orthosiphon stamineus* ethanolic leaf extract on enhancing memory in sprague dawley rats possibly via blockade of adenosine A_{2A} receptors. Evid. Based Compl. Alternative Med. 2015, 375837.

Grossberg, G.T., 2003. Cholinesterase inhibitors for the treatment of Alzheimer's disease:: getting on and staying on. Curr. Ther. Res. Clin. Exp. 64 (4), 216–235.

Heneka, M.T., Golenbock, D.T., Latz, E., 2015. Innate immunity in Alzheimer's disease. Nat. Immunol. 16 (3), 229–236.

Hossain, M.A., Mizanur Rahman, S.M., 2015. Isolation and characterisation of flavonoids from the leaves of medicinal plant Orthosiphon stamineus. Arab. J. Chem. 8 (2), 218–221.

Hsu, C.-L., Hong, B.-H., Yu, Y.-S., Yen, G.-C., 2010. Antioxidant and anti-inflammatory effects of orthosiphon aristatus and its bioactive compounds. J. Agric. Food Chem. 58 (4), 2150–2156.

Huang, X., Moir, R.D., Tanzi, R.E., Bush, A.I., Rogers, J.T., 2004. Redox-active metals, oxidative stress, and Alzheimer's disease pathology. Ann. N. Y. Acad. Sci. 1012, 153–163.

Hung, Y.N., Kadziola, Z., Brnabic, A.J., Yeh, J.F., Fuh, J.L., Hwang, J.P., Montgomery, W., 2016. The epidemiology and burden of Alzheimer's disease in Taiwan utilizing data from the national health insurance research database. Clinicoecon. Outcomes Res. 8, 387–395.

Hwang, J.-W., Choi, J.-H., Kang, S.-M., Lee, S.-G., Kang, H., 2021. Antioxidant and anti-inflammatory effects of hot water and ethanol extracts from endemic plants in Indonesia. Biomed. Sci. Lett. 27 (3), 161–169.

Ishii, M., Iadecola, C., 2015. Metabolic and non-cognitive manifestations of Alzheimer's disease: the hypothalamus as both culprit and target of pathology. Cell Metabol. 22 (5), 761–776.

Jeremic, D., Jiménez-Díaz, L., Navarro-López, J.D., 2021. Past, present and future of therapeutic strategies against amyloid-β peptides in Alzheimer's disease: a systematic review. Ageing Res. Rev. 72, 101496.

Ju Hwang, C., Choi, D.Y., Park, M.H., Hong, J.T., 2019. NF-κB as a key mediator of brain inflammation in Alzheimer's disease. CNS Neurol. Disord.: Drug Targets 18 (1), 3–10.

Kang, J.Q., 2021. Epileptic Mechanisms shared by Alzheimer's disease: viewed via the unique lens of genetic epilepsy. Int. J. Mol. Sci. 22 (13).

Kao, Y.-H., Hsu, C.-C., Yang, Y.-H., 2022. A nationwide survey of dementia prevalence in long-term care facilities in Taiwan. J. Clin. Med. 11 (6), 1554.

Khazaei, Z., Rashidi, K., Momenabadi, V., Goodarzi, E., 2021. Burden of Alzheimers Disease and Other Dementias in Elderly People in Asia A Systematic Analysis for the Global Burden of Disease Study in 2019. Ann. Med. Health Sci. Res.

Kocahan, S., Doğan, Z., 2017. Mechanisms of Alzheimer's disease pathogenesis and prevention: the brain, neural pathology, N-methyl-D-aspartate receptors, tau protein and other risk factors. Clin. Psychopharmacol. Neurosci. 15 (1), 1–8.

Kopeikina, K.J., Hyman, B.T., Spires-Jones, T.L., 2012. Soluble forms of tau are toxic in Alzheimer's disease. Transl. Neurosci. 3 (3), 223–233.

Korte, N., Nortley, R., Attwell, D., 2020. Cerebral blood flow decrease as an early pathological mechanism in Alzheimer's disease. Acta Neuropathol. 140 (6), 793–810.

Kuo, P.C., Schroeder, R.A., 1995. The emerging multifaceted roles of nitric oxide. Ann. Surg. 221 (3), 220.

Lanctôt, K.L., Amatniek, J., Ancoli-Israel, S., Arnold, S.E., Ballard, C., Cohen-Mansfield, J., Ismail, Z., Lyketsos, C., Miller, D.S., Musiek, E., 2017. Neuropsychiatric signs and symptoms of Alzheimer's disease: new treatment paradigms. Alzheimer's Dementia: Transl. Res. Clin. Intervent. 3 (3), 440–449.

Lim, J., Chua, L.S., 2021. Concentrating rosmarinic acid from Orthosiphon aristatus extract for high antioxidative candies. Ann. Univ Dunarea Jos Galati. Fasc. VI – Food Technol. 45, 118–128.

Liu, Q.F., Choi, H., Son, T., Kim, Y.M., Kanmani, S., Chin, Y.W., Kim, S.N., Kim, K.K., Kim, K.W., Koo, B.S., 2022. Co-treatment with the herbal medicine SIP3 and donepezil improves memory and depression in the mouse model of Alzheimer's disease. Curr. Alzheimer Res. 19 (3), 246–263.

Liu, T., Zhang, L., Joo, D., Sun, S.-C., 2017. NF-κB signaling in inflammation. Signal Transduct. Targeted Ther. 2 (1), 17023.

Mahdy, K., Shaker, O., Wafay, H., Nassar, Y., Hassan, H., Hussein, A., 2012. Effect of some medicinal plant extracts on the oxidative stress status in Alzheimer's disease induced in rats. Eur. Rev. Med. Pharmacol. Sci. 16 (3), 31–42.

Malekan, M., Nezamabadi, S.S., Samami, E., Mohebalizadeh, M., Saghazadeh, A., Rezaei, N., 2022. BDNF and its signaling in cancer. J. Cancer Res. Clin. Oncol. 149 (6), 2621–2636.

Mark, R.J., Hensley, K., Butterfield, D.A., Mattson, M.P., 1995. Amyloid beta-peptide impairs ion-motive ATPase activities: evidence for a role in loss of neuronal Ca2+ homeostasis and cell death. J. Neurosci. 15 (9), 6239–6249.

Mat Nuri, T.H., Hong, Y.H., Ming, L.C., Mohd Joffry, S., Othman, M.F., Neoh, C.F., 2017. Knowledge on Alzheimer's disease among public hospitals and health clinics pharmacists in the State of Selangor, Malaysia. Front. Pharmacol. 8, 739.

Medeiros, R., Baglietto-Vargas, D., LaFerla, F.M., 2011. The role of tau in Alzheimer's disease and related disorders. CNS Neurosci. Ther. 17 (5), 514–524.

Minghetti, L., 2004. Cyclooxygenase-2 (COX-2) in inflammatory and degenerative brain diseases. J. Neuropathol. Exp. Neurol. 63 (9), 901–910.

Mohd Bohari, S.P., Chua, L.S., Adrus, N., Rahmat, Z., Abdullah Al-Moalemi, H.A., 2021. Biochemical characterization of orthosiphon aristatus and evaluation of pharmacological activities. J. Herbs, Spices, Med. Plants 27 (3), 305–321.

Neniskyte, U., Neher, J.J., Brown, G.C., 2011. Neuronal death induced by nanomolar amyloid β is mediated by primary phagocytosis of neurons by microglia. J. Biol. Chem. 286 (46), 39904–39913.

Ngamrojanavanich, N., Manakit, S., Pornpakakul, S., Petsom, A., 2006. Inhibitory effects of selected Thai medicinal plants on Na+,K+-ATPase. Fitoterapia 77 (6), 481–483.
Obulesu, M., Rao, D.M., 2011. Effect of plant extracts on Alzheimer's disease: an insight into therapeutic avenues. J. Neurosci. Rural Pract. 2 (1), 056-061.
Oeckinghaus, A., Ghosh, S., 2009. The NF-κB family of transcription factors and its regulation. Cold Spring Harbor Perspect. Biol. 1 (4), a000034.
Peña-Bautista, C., Baquero, M., Vento, M., Cháfer-Pericás, C., 2019. Free radicals in Alzheimer's disease: lipid peroxidation biomarkers. Clin. Chim. Acta 491, 85–90.
Retinasamy, M.T., 2019. Evaluation of Neuroprotective Activity of Standardized Ethanolic Orthosiphon Stamineus Extract to Ameliorate Cognitive Alterations in Alzheimer's Disease. Monash University.
Retinasamy, T., Shaikh, M.F., Kumari, Y., Abidin, S.A.Z., Othman, I., 2020. Orthosiphon stamineus standardized extract reverses streptozotocin-induced Alzheimer's disease-like condition in a rat model. Biomedicines 8 (5).
Retinasamy, T., Shaikh, M.F., Kumari, Y., Othman, I., 2019. Ethanolic extract of orthosiphon stamineus improves memory in scopolamine-induced amnesia model. Front. Pharmacol. 10.
Rocha, J., Eduardo-Figueira, M., Barateiro, A., Fernandes, A., Brites, D., Bronze, R., Duarte, C.M., Serra, A.T., Pinto, R., Freitas, M., Fernandes, E., Silva-Lima, B., Mota-Filipe, H., Sepodes, B., 2015. Anti-inflammatory effect of rosmarinic acid and an extract of Rosmarinus officinalis in rat models of local and systemic inflammation. Basic Clin. Pharmacol. Toxicol. 116 (5), 398–413.
Samidurai, D., Pandurangan, A.K., Krishnamoorthi, S.K., Perumal, M.K., Nanjian, R., 2020. Sinensetin isolated from Orthosiphon aristatus inhibits cell proliferation and induces apoptosis in hepatocellular carcinoma cells. Process Biochem. 88, 213–221.
Saravanan, R., Pemaiah, B., Sridharan, S., Narayanan, M., Sivakumar, R., 2017. Enhanced cytotoxic potential of Orthosiphon stamineus extract in MCF-7 cells through suppression of nucleolin and BCL2. Bangladesh J. Pharmacol. 12, 268.
Scheltens, P., De Strooper, B., Kivipelto, M., Holstege, H., Chételat, G., Teunissen, C.E., Cummings, J., van der Flier, W.M., 2021a. Alzheimer's disease. Lancet 397 (10284), 1577–1590.
Scheltens, P., De Strooper, B., Kivipelto, M., Holstege, H., Chételat, G., Teunissen, C.E., Cummings, J., van der Flier, W.M., 2021b. Alzheimer's disease. Lancet 397 (10284), 1577–1590.
Silva, C.d., Herdeiro, R., Mathias, C., Panek, A., Silveira, C., Rodrigues, V., Rennó, M., Falcão, D., Cerqueira, D., Minto, A., 2005. Evaluation of antioxidant activity of Brazilian plants. Pharmacol. Res. 52 (3), 229–233.
Son, J.-Y., Park, S.-Y., Kim, J.-Y., Won, K.-C., Kim, Y.-D., Choi, Y.-J., Zheng, M.S., Son, J.-K., Kim, Y.-W., 2011. Orthosiphon stamineus reduces appetite and visceral fat in rats. J. Korean Soc. Appl. Biol. Chem. 54 (2), 200–205.
Sun, X., Chen, W.D., Wang, Y.D., 2015. β-Amyloid: the key peptide in the pathogenesis of Alzheimer's disease. Front. Pharmacol. 6, 221.
Tabana, Y.M., Al-Suede, F.S.R., Ahamed, M.B.K., Dahham, S.S., Hassan, L.E.A., Khalilpour, S., Taleb-Agha, M., Sandai, D., Majid, A.S.A., Majid, A.M.S.A., 2016. Cat's whiskers (Orthosiphon stamineus) tea modulates arthritis pathogenesis via the angiogenesis and inflammatory cascade. BMC Compl. Alternative Med. 16 (1), 480.
Toledo, E., Inestrosa, N., 2010. Activation of Wnt signaling by lithium and rosiglitazone reduced spatial memory impairment and neurodegeneration in brains of an APPswe/PSEN1ΔE9 mouse model of Alzheimer's disease. Mol. Psychiatr. 15 (3), 272–285.
Van Dam, D., Coen, K., De Deyn, P.P., 2008. Cognitive evaluation of disease-modifying efficacy of donepezil in the APP23 mouse model for Alzheimer's disease. Psychopharmacology 197 (1), 37–43.
Varadarajan, S., Yatin, S., Aksenova, M., Butterfield, D.A., 2000. Review: Alzheimer's amyloid beta-peptide-associated free radical oxidative stress and neurotoxicity. J. Struct. Biol. 130 (2–3), 184–208.
Viswanathan, A., Greenberg, S.M., 2011. Cerebral amyloid angiopathy in the elderly. Ann. Neurol. 70 (6), 871–880.
Vossel, K.A., Tartaglia, M.C., Nygaard, H.B., Zeman, A.Z., Miller, B.L., 2017. Epileptic activity in Alzheimer's disease: causes and clinical relevance. Lancet Neurol. 16 (4), 311–322.
Wahab, N.A.A., Chua, L.S., 2022. Partitioning phytochemicals in orthosiphon aristatus extract with antioxidant and antibacterial properties. Biointerface Res. Appl. Chem.
Weidner, W.S., Barbarino, P., 2019. P4-443: the state of the art of dementia research: new frontiers. Alzheimer's Dementia 15 (7S_Part_28). P1473-P1473.
Yang, B., Qin, J., Nie, Y., Li, Y., Chen, Q., 2017. Brain-derived neurotrophic factor propeptide inhibits proliferation and induces apoptosis in C6 glioma cells. Neuroreport 28 (12), 726–730.
Yehya, A.H.S., Asif, M., Abdul Majid, A.M.S., Oon, C.E., 2021. Complementary effects of Orthosiphon stamineus standardized ethanolic extract and rosmarinic acid in combination with gemcitabine on pancreatic cancer. Biomed. J. 44 (6), 694–708.
Zarrouk, A., Nury, T., Riedinger, J.M., Rouaud, O., Hammami, M., Lizard, G., 2015. Dual effect of docosahexaenoic acid (attenuation or amplification) on C22:0-, C24:0-, and C26:0-Induced mitochondrial dysfunctions and oxidative stress on human neuronal SK-N-BE cells. J. Nutr. Health Aging 19 (2), 198–205.
Zhang, X.X., Tian, Y., Wang, Z.T., Ma, Y.H., Tan, L., Yu, J.T., 2021. The epidemiology of Alzheimer's disease Modifiable risk factors and prevention. J. Prev. Alzheimers Dis. 8 (3), 313–321.